Single Bacteriorhodopsin Molecules Revealed on Both Surfaces of Freeze-dried and Heavy Metal-decorated Purple Membranes

DANIEL STUDER, HANS MOOR, and HEINZ GROSS
Institut für Zellbiologie, Eidgenössische Technische Hochschule, Hönggerberg, 8093 Zürich, Switzerland

ABSTRACT The flat sheets of the purple membrane from *Halobacterium halobium* contain only a single protein (bacteriorhodopsin) arranged in a hexagonal lattice. After freeze-drying at −80°C (a method that is superior to air-drying), shadowing with tantalum/tungsten, and image processing, structural details on both surfaces are portrayed in the range of 2 nm.

One surface is rough and lattice lines are clearly visible, whereas the other is smooth and the hexagonal order seems to be absent. The optical diffraction patterns, however, indicate a hexagonal lattice for both surfaces. In addition, these diffraction patterns are characteristic and easily distinguished. The orientation of the two surfaces was identified by silver decoration: partial condensation of silver on purple membranes enabled the smooth surface to be identified as the plasmatic and the rough surface as the exoplasmatic surface. After image processing, the exoplasmatic surface shows a triplet structure which exactly fits the projected structure determined by Unwin and Henderson (1975. *Nature (Lond.)*. 257:28–32) at molecular resolution, whereas, on the plasmatic surface, four image details per unit cell are visible. Three of them match the arrangement of bacteriorhodopsin, whereas the fourth must be located over a lipidic array.

Summarizing these results, it is possible to show the part of each single bacteriorhodopsin protein that is present in the surfaces of the purple membrane. By "shadowing" the membranes perpendicularly, we prove that these components of the surfaces are mainly portrayed by a decoration effect of the tantalum/tungsten condensate.

Heavy metal shadowing provides direct access to the surface structures of biological membranes. Structural resolution in the range of 2–3 nm was obtained after freeze-fracturing (8, 16, 20) and freeze-drying (15, 22), but up to now such structural details could not be correlated with known biochemical and structural data. To show that such correlation is possible and due to the abundance of existing information, we chose the purple membrane (PM) for our experiments (for review, see reference 27). This light energy-transducing membrane (24), isolated from *Halobacterium halobium* (25), consists of flat sheets in suspension (3). Bacteriorhodopsin (bR), the only protein found in PM (24), is embedded in an asymmetrical lipid bilayer (4). The lipid composition is known (18, 19), as well as the amino acid sequence of bR (7, 26). The molecules of bR form a two-dimensional crystal with a hexagonal lattice of plane group p3 (14). The structure of bR has been determined within a resolution of 7 Å (28) and the three-dimensional structure described (13). The protein contains seven α-helical segments which extend roughly perpendicular through the membrane for most of its width. To identify the exoplasmatic (E-side) and the plasmatic (P-side) surface of the three-dimensional model of bR, the PM was adsorbed with the P-side on a poly-L-lysine-coated carbon film (6). It was then examined as a frozen-hydrated specimen (11). A means of correlating the biochemical and structural data of bR was also proposed (5).

Little is known about the structural surface properties; x-ray results suggest that the surface is "smooth," with a roughness <7 Å (12), and that the crystalline order extends at least to the P-side, as has been shown by silver decoration (23, 30). A resolution <50 Å has never been achieved on the surfaces of PM, because surface preservation was insufficient (6, 29, 30). We report here that freeze-drying at −80°C allows better preservation of surface structures than air-drying. After tantalum/tungsten (Ta/W) shadowing (0.5 nm) and image proc-

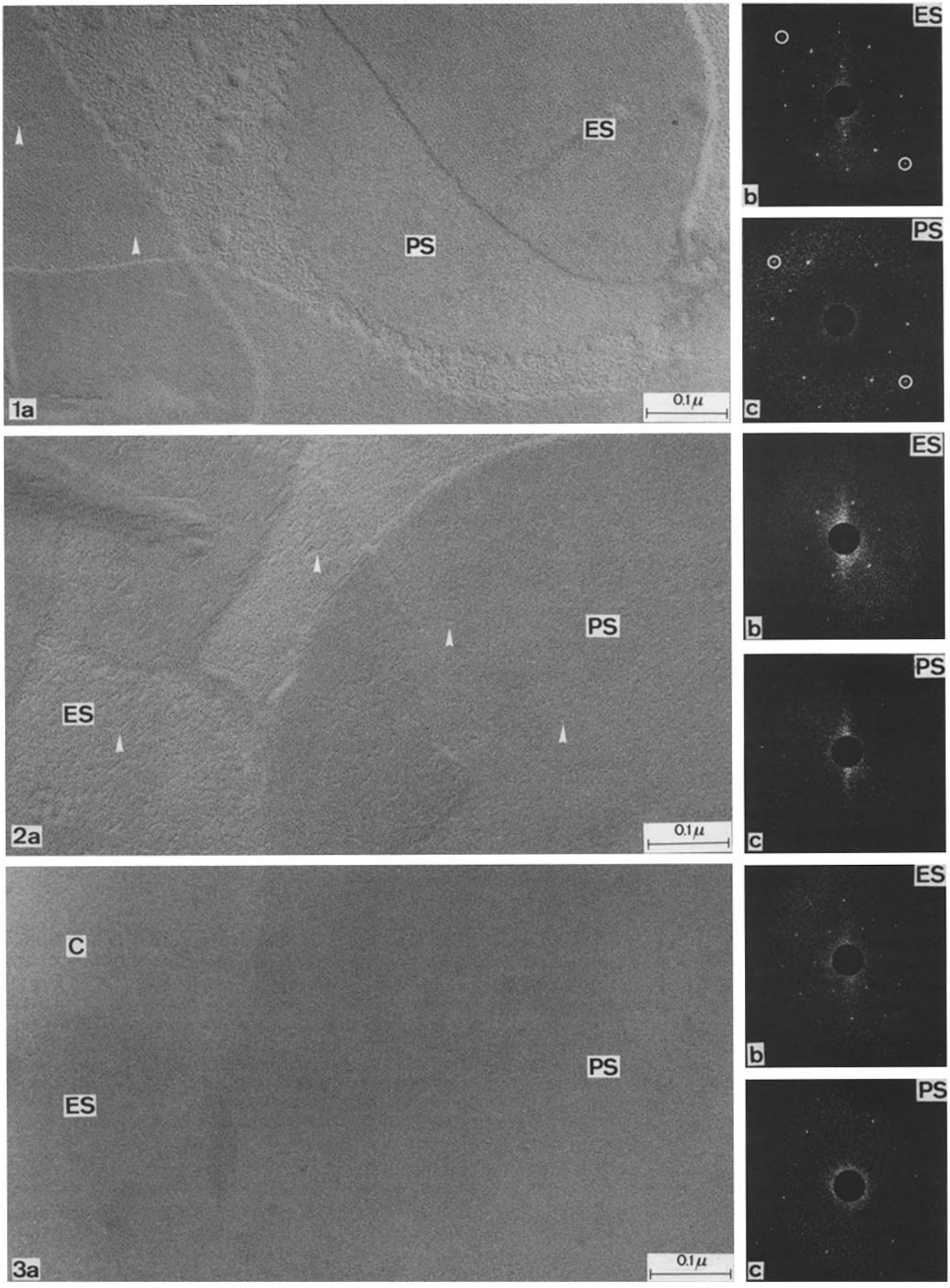

essing, single bR-molecules are visualized on both the E- and the P-side of the PM for the first time. The metal decoration effect, which leads to this portrayal, is discussed: during vacuum evaporation, the formation of a thin film proceeds via thermal accommodation, surface diffusion, nucleation, crystal growth, and crystal coalescence (1, 32). The formation of individual, more or less evenly spaced crystals is caused by the lateral mobility (surface diffusion) of the thermally accommodating metal atoms. If the surface exposes an unequal distribution of adhesion forces, nucleation and crystal growth occur mainly at places with higher binding energy (2, 9, 23). Therefore, at higher resolution this so-called decoration effect can be responsible for the revealing of structural details as well as the effect of shadow-casting.

MATERIALS AND METHODS

Purple Membranes

H. halobium cells (strain R1M1) were grown, and the PM was prepared according to published procedures (25). The membranes were stored in the dark at 5°C in twice distilled water containing 0.01% sodium azide.

Grid Preparation

5-nm-thick carbon films were obtained by evaporating carbon with an electron beam-heated evaporator (21) onto freshly cleaved mica at a pressure of 1×10^{-5} mbar in a Balzers BAF 300 device (Balzers-Union, Inc., Balzers, Liechtenstein). The films were floated on twice distilled water and picked up from underneath with 400-mesh copper grids. (The grids were cleaned beforehand by sonication in chloroform/methanol, 1:1, and 2% hydrochloric acid, then washed with twice distilled water and ethanol, and then dried.)

Specimen Preparation

Carbon-coated grids (not older than one month) were pretreated by exposure to a glow discharge at 1×10^{-1} mbar for 1 min. Such grids were brought into contact with the surface of a droplet of Alcian Blue solution (Alcian Blue 8GX p.a. C.I. 74240; Serva, Heidelberg, W. Germany, concn 5 mM) for 5–10 s, rinsed with twice distilled water for 20 s, and dried in a jet of dry nitrogen gas. Grids thus treated possess a positively charged surface which efficiently adsorbs PM. Those grids were immediately brought into contact (5–10 s) with a drop of PM suspension (5 μl, 1 mg protein/ml) and rinsed with twice distilled water.

Freeze-drying

The wet grids were put specimen-side-down on a wet filter paper in a moist chamber to prevent drying before freezing. The specimens were frozen in supercooled nitrogen at −210°C. While submersed in liquid nitrogen, four grids were fixed in a special table of the Balzers counterflow loading device. The loaded table was transferred to a Balzers BAF 300 freeze-etch unit (vented and flushed with dry nitrogen gas) and clamped into the precooled (−120°C) specimen stage. After reaching a vacuum $\leq 1 \times 10^{-6}$ mbar, the specimens were warmed up to −80°C and the liquid nitrogen–cooled microtome arm was placed over them. Under these conditions, the samples were allowed to dry. The drying procedure was finished when the water partial pressure (measured with a mass spectrometer, Balzers QMG 101) did not rise when the microtome arm was withdrawn from the specimen stage. The drying procedure lasted for ~60 min.

Air-drying

After rinsing the samples with twice distilled water, the adsorbed PM were dried for ~20 s in a stream of dry nitrogen gas (6). Then the grids were fixed on a special table and, at room temperature, transferred to the vacuum chamber. At a residual gas pressure of $< 1 \times 10^{-6}$ mbar, the liquid nitrogen–cooled microtome arm was placed over the grids and the specimen stage was cooled at −80°C.

Shadowing

The dry samples were shadowed at a temperature of −80°C with 0.5 nm Ta/W (deposition rate 0.1 nm/sec) at an angle of 45° or 90° and afterward coated perpendicularly with a 5-nm-thick carbon layer. For perpendicular silver evaporation, a hole was drilled in the carbon electrode of the electron beam-heated evaporator and then filled with a small piece of silver wire ($\phi = 1$ mm). By using a shutter, it was possible to deposit perpendicularly 0.6 nm of silver onto the specimens. Subsequently, the specimens were shadowed with 0.5 nm Ta/W at an angle of 45°; a final layer of 5 nm of carbon was added to reduce alterations of the thin metal films after deposition (1).

Film thickness and deposition rate were measured with a quartz-crystal thin-film monitor (Balzers QSG 201) and a rate meter (Balzers QRG 201). Exactly reproducible values of film thickness were achieved by the use of a deposition-controlled, pneumatically-driven shutter. After shadowing, the freeze- and air-dried specimens were warmed up to +20°C *in vacuo* and afterward examined in the electron microscope or stored in a desiccator at 1×10^{-1} mbar. To minimize film alterations such as grain migration and recrystallization (1, 23), the specimens were examined within 12 h.

Electron Microscopy

In a Siemens Elmiskop 102 equipped with an anticontamination device, the specimens were examined at 100 kV at a magnification of × 50,000. The magnification was calibrated with negatively stained catalase (Balzers-Union). Agfa-Gevaert Scientia electron microscopic film was used.

Optical Diffraction and Image Processing

The micrographs were used directly for producing optical diffraction patterns which were recorded on 35-mm film (Ilford, Inc., Fribourg, Switzerland). Image processing (17) was carried out by digitizing copies of the micrographs with an optronics P-1700 photoscan/photowrite unit (Optronics International, Inc. Chelmsford, Mass.) having 8 bit density resolution. The scan spot size was 25 × 25 μm^2, which corresponds to 0.5 × 0.5 nm^2 at the magnification of the micrographs (× 50,000). Fourier transforms of 256 × 256 picture elements were computed. The geometrical arrangement of the largest 300 Fourier intensities was printed out. The diffraction pattern was indexed from this display. Optimal reciprocal lattice vectors (determining "the filter holes"), together with the highest admissible order (4), were entered into an inverse Fourier filtering routine. All Fourier coefficients inside the "filter-holes" (3 × 3 picture elements) were computed without change. Their intensities were recorded and reconverted in a photographic representation using the photowrite.

RESULTS

Surface Structures and Optical Diffraction Patterns

PM freeze-dried and shadowed with Ta/W at an angle of 45° show several surface features (Fig. 1 *a*). In the upper right corner of Fig. 1 *a* a folded-over membrane is shown. Conse-

FIGURE 1 PM freeze-dried at −80°C and tantalum/tungsten (Ta/W) shadowed (*a*) at an angle of 45° distinguish between the "rough" E-side (*ES*) and the "smooth" P-side (*PS*). The arrows indicate the cracks that occur when the PS is directly adsorbed on the Alcian Blue–treated carbon film. The characteristic diffraction patterns of the *ES* (*b*, the six spots that are the same distance from the center as spot [1,1] are very strong) and the *PS* (*c*, strong second-order spots) are shown. The encircled spots indicate a resolution of 2 nm. Magnification for Figs. 1–4: × 150,000. Magnification for diffraction patterns of Figs. 1–4: 1 cm ≅ 3.4 nm.

FIGURE 2 The air-dried PM (*a*) show cracks (*ES*, arrows) on one side and dimples (*PS*, arrows) on the other side. The cracked surface shows first-order spots in the optical diffraction pattern (*b*), whereas on the dimpled surface no distinct spots (*c*) are depicted.

FIGURE 3 Freeze-dried PM shadowed perpendicularly with Ta/W: no prominent structures are obvious. "C" labels a region where only the Alcian Blue–treated carbon film is visible. On the *ES*, weak-lattice lines can be detected. The diffraction patterns (*b* and *c*), however, are analogous to those of Fig. 1 *b* and *c*.

quently, both the P-side and the E-side are exposed. The overlapping part shows straight lines indicating a lattice structure (rough side), whereas the surface of the part adsorbed directly onto Alcian Blue–coated carbon film seems to be amorphous (smooth side). On the left side of Fig. 1 *a*, another rough surface with small cracks (arrows) is shown. Consequently, these cracks result from an adsorption artifact which appears only when the smooth surface is directly adsorbed on Alcian Blue. The rough side in the upper right corner of the picture does not show cracks, probably because the smooth side is adsorbed on the smooth part of an underlying membrane. According to the literature (6, 30), the cracks indicate that the rough surface is identical with the E-side. Also, the optical diffraction patterns allow differentiation between the rough and the smooth side, whereas on the diffraction pattern of the rough surface (Fig. 1 *b*), all six first-order spots and their vectorial addition appear very strong, the pattern of the smooth surface (Fig. 1 *c*) is characterized by weak or absent first-order and strong second-order spots. The encircled spots of both diffraction patterns indicate a resolution of 2 nm.

Air-dried PM show pronounced cracks or dimples and few structural details on their surfaces (Fig. 2 *a*). The cracks obviously follow the lattice lines (forming edges with angles of 120° and 60°). They are characteristic only for one side, probably the E-side, and they are more emphasized on the part of the membrane adsorbed directly on the Alcian Blue–treated carbon film than on the part adsorbed on the dimpled membrane surface, which probably represents the P-side (6, 30). Optical diffraction patterns of the cracked surface show first-order spots (Fig. 2 *b*) and those of the dimpled one (Fig. 2 *c*) no lattice spots.

Usually, uni-directionally shadowed specimens show diffraction patterns that indicate the shadowing direction by extended and more intensive reflections in one direction (8, 15). After freeze-drying and Ta/W shadowing, the diffraction spots of the rough (Fig. 1 *b*) and the smooth surface (Fig. 1 *c*) have approximately the same intensities in all directions. This suggests a decoration effect rather than a real shadow-cast. As a proof, the membranes were "shadowed" perpendicularly (Fig. 3 *a*): such a specimen lacks shadow contrast, and therefore structures are practically invisible. Only the rough surface shows very weak lattice lines. However, the optical diffraction patterns of the rough side (Fig. 3 *b*) and of the smooth side (Fig. 3 *c*) show the same characteristic patterns as after shadowing at 45° (Fig. 1 *b* and *c*).

Membrane Surface Identification

The cracks that are revealed on only one surface of the PM indicate that the rough surface corresponds to the E-side (6, 30). To conclusively identify both membrane surfaces, silver decoration (23) was applied. On the rough side (Fig. 4 *a*), the silver grains are randomly distributed. This fact is illustrated by the diffraction pattern (Fig. 4 *c*) of the silver-shadowed part of the surface. To confirm that the surface is indeed the rough

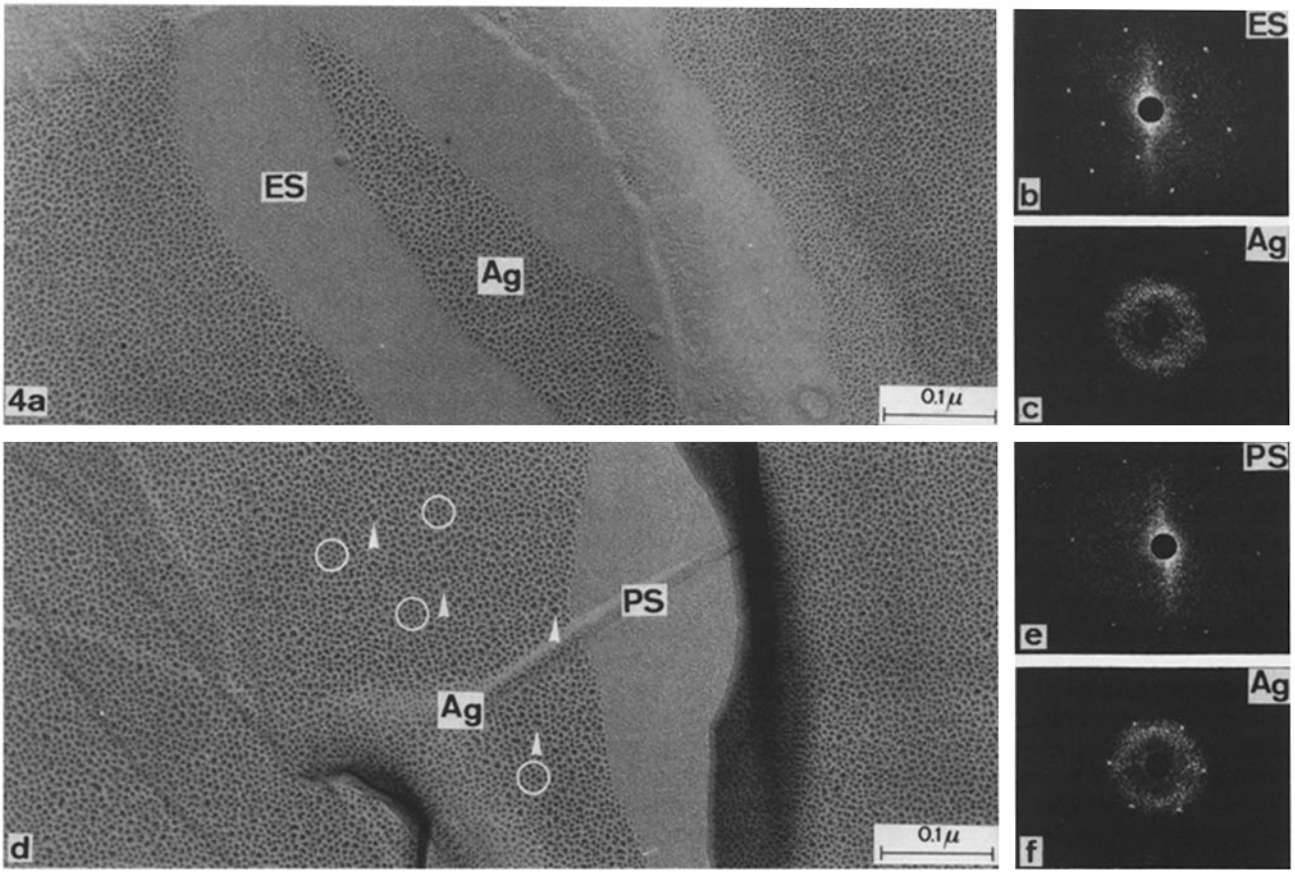

FIGURE 4 An *ES* partially shadowed with silver (*a*) exhibits randomly distributed silver grains. The characteristic diffraction patterns of the Ta/W-shadowed (*b*) and the silver-shadowed (c) part confirm that it is the *ES* on which the random distribution of the silver grains occurs. The partially silver-shadowed *PS* (*d*) shows hexagonally-ordered silver grains (very visible in the encircled areas). The arrows point to bigger silver crystallites which disturb the visual appearance of the hexagonal order. The diffraction patterns of the Ta/W- (e) and silver-shadowed (*f*) *PS* confirm that hexagonal ordering of the silver grains takes place.

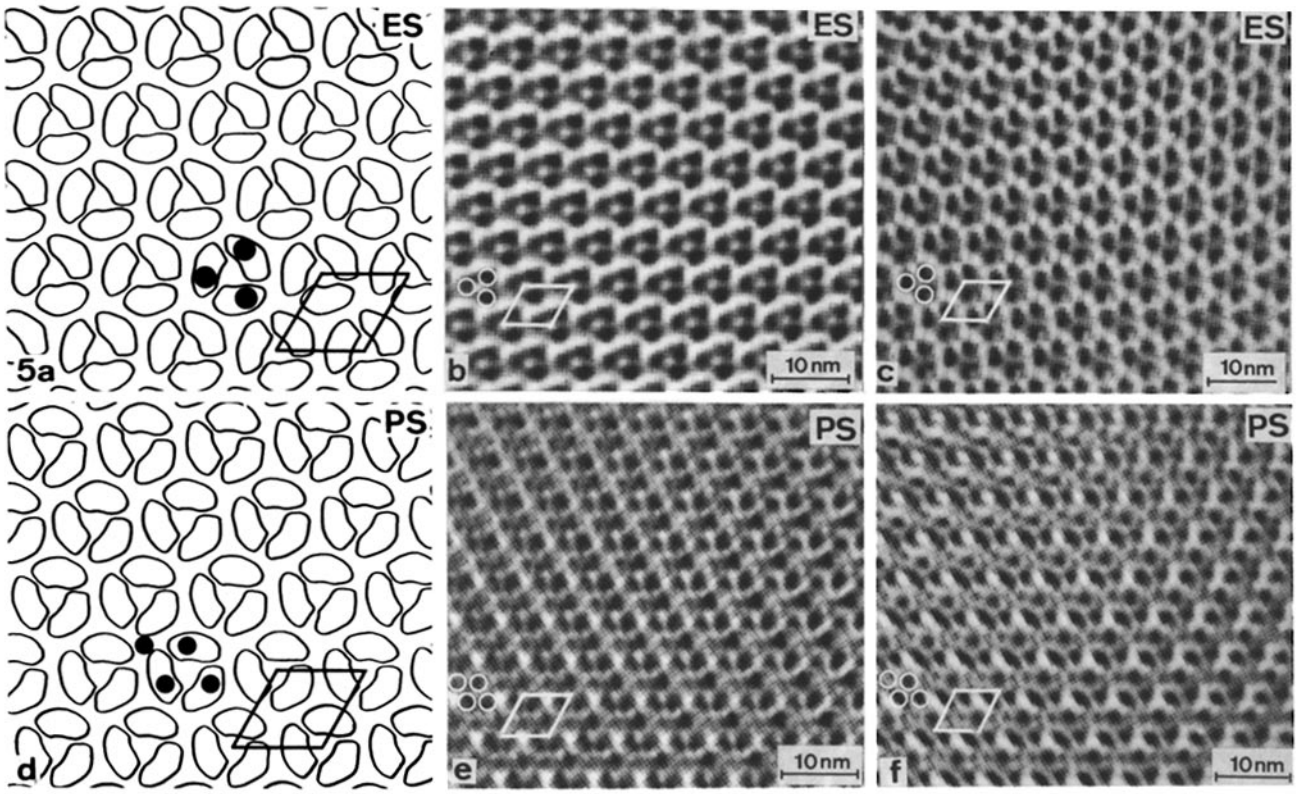

FIGURE 5 Image-processed pictures of the *ES* (*b*, shadowing angle 45°; *c*, shadowing angle 90°) show a triplet structure. The black spots (including the circled spots) indicate individual metal crystallites decorating individual bacteriorhodopsin (bR) molecules. The image processed pictures of the P-side (*e*, shadowing angle 45°; *f*, shadowing angle 90°) show four crystallites per unit cell (indicated by a rhombus), three of which decorate the bR molecules, whereas the fourth is located over a lipidic zone. The scheme of the ES (*a*) and the PS (*b*) (mirror images: derived from the model published by Unwin and Henderson [28]) are shown in order to illustrate the position of the metal crystallites (black spots) in relation to the bR trimers.

side, the accompanying diffraction pattern (Fig. 4 *b*) of the only Ta/W-shadowed part is shown. On the other hand, the silver grains on the smooth surface are hexagonally ordered (Fig. 4 *d*). The hexagonal order is directly visible only in the circled areas. Otherwise, order is not evident, because coalescence of several silver grains may form larger aggregates (arrows), which need not be necessarily placed at lattice points. Nevertheless, the grains are mainly hexagonally ordered, as shown by the optical diffraction pattern (Fig. 4 *f*) obtained from the silver-covered part of the membrane. The exclusively Ta/W-shadowed part of the same surface shows the characteristic diffraction pattern (Fig. 4 *e*) of the smooth side. According to data about silver decoration (23, 30), the smooth surface corresponds to the P-side and the rough one to the E-side.

The finding of membrane areas covered only partially with silver has been a matter of chance: it depends on partial adsorption of the membranes on the Alcian Blue–coated carbon film. During freeze-drying, such membranes build small "bridges" which are stable during shadowing. Because silver is shadowed perpendicularly, and Ta/W at an angle of 45°, there are areas below a "bridge" where only Ta/W is condensed. In the electron beam of the microscope, these "bridges" collapse and fortunately enable partially shadowed membranes to be observed. During air-drying, such bridges never have been detected, and no partially shadowed membranes were found.

Image Processing

Because only first-order spots were found, air-dried PM have not been image processed: first-order spots give only information about the basic lattice. Digital image processing of the freeze-dried PM surfaces was applied to facilitate assessing the quality of the structural record.

Fourier filtration of freeze-dried shadowings at an angle of 45° (Fig. 5 *b*) or 90° (Fig. 5 *c*) results in the record of a nearly identical triplet structure, if E-side pictures are compared: each black spot refers to one Ta/W crystallite. The triplet structure can easily be correlated with the mirror image (Fig. 5 *a*) of the scheme of Unwin and Henderson (28). (The density map reveals the projected distribution of the bR molecules viewed from the P-side.) In the scheme of the E-side (Fig. 5 *a*), each single bR is shown. In addition, a unit cell is marked by a rhombus, and the most probable position of the heavy metal crystallites is indicated by black spots. In the scheme of the P-side (Fig. 5 *d*, which represents the mirror picture of Fig. 5 *a*), the unit cell and the most probable position of the crystallites are indicated in the same way. The P-side, shadowed either at 45° (Fig. 5 *e*) or at 90° (Fig. 5 *f*), shows four metal crystallites per unit cell. Three of the metal grains decorate probably single bR molecules, and, consequently, the fourth crystallite is located over a lipidic array. An explanation of why four Ta/W crystallites per unit cell can be found, in spite of a relatively poor optical diffractogram, is as follows: if we consider the diffractograms of P-sides (Figs. 1 *c* and 3 *c*), it is a matter of fact that the second-order spots are much more intensive than those of the first order and their additions. If Fourier coefficients of only second-order spots were used to generate a processed image, one would get a basic lattice with a vector of 3.1 nm that is half of the lattice vector of the unit cell of PM.

(Each basic lattice shows only one black spot per unit cell.) One unit cell of PM would therefore correspond to 4 unit cells of the smaller lattice; hence, we get four black spots per unit cell of the PM.

DISCUSSION

Membrane Preservation and Surface Structures

The structural details shown on freeze-dried PM surfaces are of the same size as the Ta/W crystallites (1.5–2 nm) which are used for their visualization. We infer from this that the obtained structural resolution is limited by the size of the metal crystallites. Therefore the amount of metal condensed on the surface is an important factor. If shadowing is done with too much metal, the crystallites enlarge and coalesce, resulting in a loss of resolution. Shadowing with too little metal renders the observation of the specimens in the microscope very difficult. 0.5 nm of Ta/W seems to be about the optimal film thickness for the resolution of the portrayed structures. Data about the resolution power of the most conventional shadowing materials, such as platinum/carbon (Pt/C) and Ta/W, is of interest for many applications. Currently, we are engaged in the comparison of Pt/C and Ta/W, testing factors such as film thickness on the record of freeze-dried PM surfaces. Our findings in this direction will be presented elsewhere. Here we have chosen Ta/W results because it was repeatedly demonstrated that Ta/W films are less granular than Pt/C films (10, 31).

As already mentioned, air-dried specimens exhibit fewer structural details. In such specimens, the adsorption artifacts (cracks), also visible after freeze-drying, are drastically enhanced if the membrane is directly adsorbed on the Alcian Blue–coated carbon film. The absence of higher than first-order spots in the optical transforms proves that periodic surface features are disturbed.

Ta/W Decoration and Image Processing

We suggest that in freeze-dried specimens, the bR molecule is decorated by Ta/W for the following reasons: the probability that decoration occurs on identical surface structures is greater than the probability that it occurs on differing ones. In one unit cell, three identical surface spots can be expected which are formed by three bR molecules. The surrounding lipids are heterogeneous (19) and possibly arranged in clusters. The probability that the lipids are capable of forming just three identical clusters with the same arrangement as bR is very unlikely. Therefore, we conclude that the protein is decorated and visualized on both surfaces of the membrane. Consequently, we postulate that the fourth crystallite per unit cell on the P-side, which does not represent an expected feature, is located over a lipidic array. This additional site is the only difference between the E- and P-side. Therefore, it could be identical with the decoration site, which is responsible for the hexagonally-ordered silver condensate.

The image processed pictures of perpendicularly and obliquely shadowed E-sides are more or less identical; however, the surfaces shadowed at 45° exhibit crystallites of different size in the triplet. We consider that this phenomenon has to be explained as an effect of self-shadowing of the growing crystallites. Under such conditions, crystallites with a diameter of 1.5–2 nm are produced. The crystallites produced by perpendicular shadowing are smaller and equal in size; they show a diameter of ~1.5 nm. Because approximately the same amount of metal is deposited, more crystallites must be created and less of them can be hexagonally arranged and finally portrayed by image processing. This suggestion is supported by the following observations: the lattice lines are hardly detectable and the reflections of the diffraction patterns are weak in relation to the background.

To summarize, we conclude the following: the E- and P-sides of the PM are distinguishable at a structural resolution level of 2 nm. Although, after image processing, the E-side exactly fits the internal arrangement of the bR molecules, surprisingly, the P-side depicts an additional fourth metal crystallite located over a lipidic array. In addition, we have shown that image details originate mainly from a metal decoration effect and that freeze-drying compared to air-drying allows much better preservation of surface structures.

We wish to thank Dr. O. Kübler and Mrs. V. Vogt for their help during production of the digital filtered images; Dr. U. Müller for supplying the *Halobacterium halobium* cells; Mr. A. Frey for his excellent technical assistance; and Dr. F. Jay for her help with our English.

These studies were supported by Swiss National Science Foundation, grant No. 3.529-0.79, and predoctoral ETH-training grant No. 0.330.080.35/9.

Received for publication 29 December 1980, and in revised form 12 March 1981.

REFERENCES

1. Bachmann, L., and H. Hilbrand. 1966. Sinterung von Aufdampfschichten aus Silber und Gold unter dem Einfluss von Adsorptionsschichten. *In* Basic Problems in Thin Film Physics. Vandenhoeck and Rupprecht, Göttingen. 87–92.
2. Bassett, G. A. 1958. A new technique for decoration of cleanage and slip steps on ionic crystal surfaces. *Phil. Mag.* 3:1042–1045.
3. Blaurock, A., and W. Stoeckenius. 1971. Structure of the purple membrane. *Nat. New Biol.* 233:152–155.
4. Blaurock, A. E., and G. I. King. 1977. Asymmetric structure of purple membrane. *Science (Wash. D.C.).* 196:1101–1104.
5. Engelmann, D. M., R. Henderson, A. D. McLachlan, and B. A. Wallace. 1980. Path of the polypeptide in bacteriorhodopsin. *Proc. Natl. Acad. Sci. U. S. A.* 77:2023–2027.
6. Fisher, K. A., K. Yanagimoto, and W. Stoeckenius. 1978. Oriented adsorption of purple membrane to cationic surfaces. *J. Cell. Biol.* 77:611–621.
7. Gerber, G. E., R. J. Anderegg, W. C. Herlihy, C. P. Gray, K. Biemann, and H. G. Khorana. 1979. Partial primary structure of bacteriorhodopsin: sequencing methods for membrane proteins. *Proc. Natl. Acad. Sci. U. S. A.* 76:227–231.
8. Gross, H., E. Bas, and H. Moor. 1978. Freeze-fracturing in ultrahigh vacuum at −196°C. *J. Cell. Biol.* 76:712–728.
9. Gross, H., O. Kuebler, E. B. Bas, and H. Moor. 1978. Decoration of specific sites on freeze-fractured membranes. *J. Cell. Biol.* 79:646–656.
10. Gross, H. 1980. Ultrahigh vacuum freeze-fracturing at −196°C and decoration of specific sites of paracrystalline membranes. *In* Electron Microscopy at Molecular Dimension. Springer Verlag, Berlin. 71–79.
11. Hayward, B. S., D. A. Grano, R. M. Glaeser, and K. A. Fischer. 1978. Molecular orientation of bacteriorhodopsin within the purple membrane of *Halobacterium halobium*. *Proc. Natl. Acad. Sci. U. S. A.* 75:4320–4324.
12. Henderson, R. 1975. The structure of the purple membrane from *Halobacterium halobium*: analysis of the X-ray diffraction pattern. *J. Mol. Biol.* 93:123–138.
13. Henderson, R., and P. N. T. Unwin. 1975. Three dimensional model of purple membrane obtained by electron microscopy. *Nature (Lond.).* 257:28–32.
14. Holser, W. T. 1958. Point groups and plane groups in a two-sided plane and their subgroups. *Z. Kristallographie.* 110:266–281.
15. Kistler, J., U. Aebi, and E. Kellenberger. 1977. Freeze-drying and shadowing a two dimensional periodic specimen. *J. Ultrastruct. Res.* 59:76–85.
16. Kuebler, O., and H. Gross. 1978. UHV freeze-fracturing and image processing applied to the purple membrane. Proceedings of the Ninth International Congress on Electron Microscopy. 2:142–143.
17. Kuebler, O., H. Gross, and H. Moor. 1978. Complementary structures of membrane fracture faces obtained by UHV-freeze-fracturing at −196°C and digital image processing. *Ultramicroscopy.* 3:161–168.
18. Kushwaha, S., M. Kates, and W. G. Martin. 1975. Characterization and composition of the purple and red membrane from *Halobacterium cutirubrum*. *Can. J. Biochem.* 53:284–292.
19. Kushwaha, S., M. Kates, and W. Stoeckenius. 1976. Comparison of purple membrane from *Halobacterium cutirubrum* and *Halobacterium halobium*. *Biochim. Biophys. Acta.* 426: 703–710.
20. Moor, H. 1971. Recent progress in the freeze-etching technique. *Philos. Trans. R. Soc. Lond. B Biol. Sci.* 261:121–131.
21. Moor, H. 1970. High resolution shadow casting by the use of an electron gun. Proceedings of the Seventh International Congress Electron Microscopy. 1:413–414.
22. Nermut, M. V., and H. Frank. 1971. Fine structure of influence A2 (Singapore) as revealed by negative staining, freeze-drying and freeze-etching. *J. Gen. Virol.* 10:37–51.
23. Neugebauer, D.-C., and H. P. Zingsheim. 1978. The two faces of purple membrane: structural differences revealed by metal decoration. *J. Mol. Biol.* 123:235–246.
24. Oesterhelt, D., and W. Stoeckenius. 1971. Rhodopsin-like protein from the purple membrane of *Halobacterium halobium*. *Nat. New Biol.* 233:149–152.

25. Oesterhelt, D., and W. Stoeckenius. 1974. Isolation of the cell membrane of *Halobacterium halobium* and its fractionation into red and purple membrane. *Methods Enzymol.* 31:667–678.
26. Ovchinnikov, Y., N. Adbulaev, M. Feigiva, A. Kiselev, and N. Lobanov. 1979. The structural basis of the functioning of bacteriorhodopsin: an overview. *FEBS (Fed. Eur. Biochem. Soc.) Lett.* 100:219–224.
27. Stoeckenius, W., R. M. Lozier, and R. A. Bogomolni. 1979. Bacteriorhodopsin and the purple membrane of *Halobacteria. Bioch. Biophys. Acta.* 505:215–278.
28. Unwin, P. N. T., and R. Henderson. 1975. Molecular structure determination by electron microscopy of unstained crystalline specimens. *J. Mol. Biol.* 94:425–440.
29. Usukura, J., E. Yamada, F. Tokunada, and T. Yoshizawa. 1980. Ultrastructure of purple membrane and cell wall of *Halobacterium halobium. J. Ultrastruct. Res.* 70:204–219.
30. Zingsheim, H. P., R. Henderson, and D.-C. Neugebauer. 1978. Properties of the two sides of the purple membrane correlated. *J. Mol. Biol.* 123:275–278.
31. Zingsheim, H. P. 1972. Membrane structure and electron microscopy. The significance of physical problems and techniques (Freeze-Etching). *Biochim. Biophys. Acta.* 265:339–366.
32. Zinsmeister, G. 1973. Present status of the theory of thin film condensation. *Vacuum-Technik.* 22:85–93.